# Solution Chemistry of Chalcohalide Hexanuclear Rhenium Cluster Monoanions: Substitution Reactions and Structural and LSIMS Characterization of the Heterosubstituted Cluster Dianions, $(n\text{-}Bu_4N)_2[Re_6Q_5ECl_8]$ (Q = S, E = O, S, Se; Q = Se, E = S, Se, Te)

**Santiago Uriel,[†] Kamal Boubekeur,[†] Patrick Batail,*[,†] Jesus Orduna,[‡] and Enric Canadell[§]**

Laboratoire de Physique des Solides, Unité Associée au CNRS No. 2, Université de Paris-Sud, 91405 Orsay, France, Instituto de Ciencia de Materiales de Aragon, Universidad de Zaragoza, 50009 Zaragoza, Spain, and Laboratoire de Chimie Théorique, Unité Associée au CNRS No. 506, Université de Paris-Sud, 91405 Orsay, France

*Received January 13, 1995*[⊗]

The gentle, efficient, and specific substitution of one face-bridging inner chloride ligand ($Cl^i$) upon reaction of $(n\text{-}Bu_4N)[Re_6Q^i_5Cl^i_3(Cl^a_6)]$ (Q = S, Se) with $[(CH_3)_3Si]_2E$ (E = O, S, Se, Te) reagents provides at room temperature and in high yields the tetrabutylammonium salts of the chalcogen-enriched, eventually heterosubstituted, hexanuclear molecular cluster dianions $(n\text{-}Bu_4N)_2[Re_6S^i_5E^iCl^i_2(Cl^a_6)]$ (E = O, **1**; S, **2**; Se, **3**) and $(n\text{-}Bu_4N)_2[Re_6Se^i_5E^iCl^i_2(Cl^a_6)]$ (E = S, **4**; Se, **5**; Te, **6**). The latter have been fully characterized by liquid secondary negative ion mass spectrometry (LSIMS). The crystal structures of $(n\text{-}Bu_4N)_2Re_6S_5OCl_8$ and $(n\text{-}Bu_4N)_2Re_6Se_5TeCl_8$ have been determined. Crystal data for **1**: $P2_1/a$, $a = 18.377(1)$ Å, $b = 16.138(6)$ Å, $c = 18.257(3)$ Å, $\beta = 92.16(1)°$, $V = 5410(2)$ Å$^3$, $Z = 4$. Crystal data for **6**: $P2_1/n$, $a = 12.877(2)$ Å, $b = 11.312(8)$ Å, $c = 18.613(3)$ Å, $\beta = 90.11(1)°$, $V = 2711(2)$ Å$^3$, $Z = 2$. There is a significant contraction of the single octahedron face capped by the oxygen atom in the oxo sulfido rhenium cluster $[Re_6S_5OCl_8]^{2-}$. The values of the Re–$Cl^a$ distances in both structures complement earlier structural studies and confirm that this distance increases with the molecular cluster charge. Molecular orbital calculations of the extended Hückel type for the series of model molecular clusters $Re_6S^i_4Cl^i_4(Cl_6)$, $[Re_6S^i_5Cl^i_3(Cl^a_6)]^-$, $[Re_6S^i_6Cl^i_2(Cl^a_6)]^{2-}$, $[Re_6S^i_7Cl^i(Cl^a_6)]^{3-}$, and $[Re_6S^i_8(Cl^a_6)]^{4-}$, as well as $[Re_6S^i_5O^iCl^i_2(Cl^a_6)]^{2-}$, demonstrate that the thermalized average Re–$Cl^a$ overlap population decreases with the increase in cluster charge, a genuine electronic effect which supports the conclusion that the actual Re–$Cl^a$ distances in a given structure is specific of the cluster anion charge. The shrinking of the oxo-capped $Re_3$ face on the contrary is not an electronic effect but is more the result of a steric adjustment.

## Introduction

Recent developments in the solution chemistry of molecular forms of hexanuclear chalcohalide rhenium clusters have revealed that the cluster monoanions, $[Re_6Q^i_5Cl^i_3(Cl^a_6)]^-$, (Q = S, Se), (where i stands for an inner ligand capping a face of the $Re_6$ octahedron and a for an apical, terminal ligand linked to a single rhenium atom), readily transform at moderate temperature (ca. 50 °C) into the chalcogen-enriched dianions, $[Re_6Q^i_6Cl^i_2(Cl^a_6)]^{2-}$.[1] Similar cluster core reactions (which involve face-capping $L^i$ ligands) have also been described in parallel work by Holm et al., who demonstrated that $Re_6Se_5Cl_9^-$ reacts with $Li_2Se$ to give $Re_6Se_6Cl_8^{2-}$ and that treatment of $Re_6Se_4Cl_{10}$ in DMF/$H_2O$ at 70 °C yields $Re_6Se_4O_2Cl_8^{2-}$.[2] While these initial reactivity studies all suggest the cluster dianions to be the thermodynamically most stable molecular forms of these hexanuclear rhenium clusters, they remain of little synthetic potential since the thermal conversion proceeds in very low yields and the latter two reactions also suffer from very low yields and a poor control of the high temperature synthesis of $Re_6Se_4Cl_{10}$ which does not give a single phase material.

In this paper, we report our investigation of the reactions (Scheme 1) of $(n\text{-}Bu_4N)[Re_6Q^i_5Cl^i_3(Cl^a_6)]$, (Q = S, Se), with

**Scheme 1**

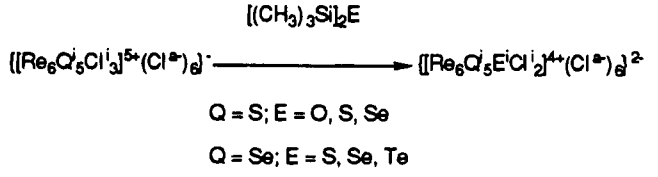


$[(CH_3)_3Si]_2E$, (E = O, S, Se, Te) reagents, that demonstrate neat, specific substitution of one inner face-bridging chloride core ligand ($Cl^i$). The reaction proceeds readily at room temperature in high yields and affords a unique series of heterosubstituted rhenium cluster dianions, i.e. with three different ligands sharing the eight face-capping ($L^i$) sites of the octahedral motif, $(n\text{-}Bu_4N)_2[Re_6Q^i_5E^iCl^i_2(Cl^a_6)]$ (Q = S, E = O, S, Se; Q = Se, E = S, Se, Te). This set of core substitution reactions represents a novel, general entry into the chemistry of these rhenium cluster dianions that complements the direct high temperature synthetic route that proceeds in high yields to give the alkaline-earth salts $CaRe_6Q_6Cl_8$ and $MgRe_6Q_6Cl_8$[3] but which is not suitable for preparing heterosubstituted cluster cores. The reactions described in this work extends the scope of the synthetic potential of such bis(trimethylsilyl) reagents as molecular sources of heteroatoms, including oxygen, toward the modification of metal clusters under mild conditions. Indeed, while $[(CH_3)_3Si]_2E$, (E = S, Se, Te), have recently been used to generate large multinuclear aggregates of group I metals from

[†] Laboratoire de Physique des Solides. Present address: Institut des Matériaux de Nantes, Unité Mixte de Recherche CNRS-Université de Nantes No. 110, 2, rue de la Houssinière, 44072 Nantes 03, France.
[‡] Instituto de Ciencia de Materiales.
[§] Laboratoire de Chimie Théorique.
[⊗] Abstract published in *Advance ACS Abstracts*, September 15, 1995.

(1) Gabriel, J.-C.; Boubekeur, K.; Batail, P. *Inorg. Chem.* **1993**, *32*, 2894-2900.
(2) Yaghi, O. M.; Scott, M. J.; Holm, R. H. *Inorg. Chem.* **1992**, *31*, 4778.
(3) Uriel, S.; Boubekeur, K.; Gabriel, J.-C.; Batail, P.; Orduna, J. To be submitted for publication.

0020-1669/95/1334-5307$09.00/0 

simple metal halides,[4] examples are scarce, however, of the use of $[(CH_3)_3Si]_2O$ in coordination or organometallic chemistry.[5]

The tetrabutylammonium salts of these novel, heterosubstituted rhenium cluster dianions have been fully characterized by liquid secondary ion mass spectrometry (LSIMS). Analyses of the crystal structures of $(n\text{-}Bu_4N)_2Re_6S_5OCl_8$ and $(n\text{-}Bu_4N)_2Re_6Se_5TeCl_8$ revealed a distortion of the $Re_6$ core for the oxo sulfido rhenium cluster, not found for the mixed chalcogen cluster, and confirm that the $Re-Cl^a$ distances increase with cluster charge, two important structural features that prompted an investigation of the electronic structure of these hexanuclear chalcohalide rhenium clusters and their heterosubstituted derivatives, based on molecular orbital calculations.

## Results and Discussion

**Efficient Room Temperature Substitution Reactions.** All reactions proceed readily in acetonitrile solutions at room temperature. The course of the reactions is conveniently monitored by observing the suspension of the only moderately soluble tetrabutylammonium salts, $(n\text{-}Bu_4N)Re_6Q_5Cl_9$, gradually turn into a clean, limpid solution of the highly soluble rhenium cluster dianions, which do not precipitate upon addition of *n*-$Bu_4NCl$. High quality single crystals of $(n\text{-}Bu_4N)_2[Re_6S^i_5O^iCl^i_2(Cl^a_6)]$, **1**; $(n\text{-}Bu_4N)_2[Re_6S^i_5S^iCl^i_2(Cl^a_6)]$, **2**; $(n\text{-}Bu_4N)_2[Re_6S^i_5Se^iCl^i_2(Cl^a_6)]$, **3**; $(n\text{-}Bu_4N)_2[Re_6Se^i_5S^iCl^i_2(Cl^a_6)]$, **4**; $(n\text{-}Bu_4N)_2[Re_6Se^i_5Se^iCl^i_2(Cl^a_6)]$, **5**; and $(n\text{-}Bu_4N)_2[Re_6Se^i_5Te^iCl^i_2(Cl^a_6)]$, **6** are obtained in high yields after evaporation of the solvent, followed by washing with ethanol and recrystallization in acetonitrile.

It is important to note that, with the exception of the reactions of $[(CH_3)_3Si]_2Te$ with the sulfido rhenium cluster discussed below, the substitution of more than one inner $Cl^i$ ligand of the rhenium cluster monoanions is never observed, despite the use of a large excess of $[(CH_3)_3Si]_2E$. This suggests that the major driving force for the reactions is to reach the cluster dianions. This is supported also by the observation that the cluster dianions themselves do not react with $[(CH_3)_3Si]_2E$ under the same conditions. Likewise, neither the mono- nor the dianion cluster forms are prone under similar conditions to substitution of one inner chloride with $[(CH_3)_3Si]SCH_3$, which indeed would leave the net cluster charge unchanged. Thus, the convenient elimination of $(CH_3)_3SiCl$ appears to be at least partly responsible for the clean reaction and ready obtention of a single solid product.

**$(n\text{-}Bu_4N)_2[Re_6S_5TeCl_8]$ and $(n\text{-}Bu_4N)_3[Re_6S_5Te_2Cl_7]$.** The particular case of the reactions of $(n\text{-}Bu_4N)Re_6S_5Cl_9$ with $[(CH_3)_3Si]_2Te$ warrant special comment. The LSIMS obtained from the solid, polycrystalline product of the room temperature reaction presents a series of peaks which were assigned by comparison of the observed and calculated isotopic ion distributions.[6] Clearly, the occurrence of the peaks at $m/z = 1747$ and 1712 indicate that double substitution has also occurred on the cluster core to give a mixture of two compounds, $(n\text{-}Bu_4N)_2[Re_6S_5TeCl_8]$ and $(n\text{-}Bu_4N)_3[Re_6S_5Te_2Cl_7]$, the monosubstituted dianion being present in larger amounts.[6] When the reaction is conducted in refluxing acetonitrile, the most intense

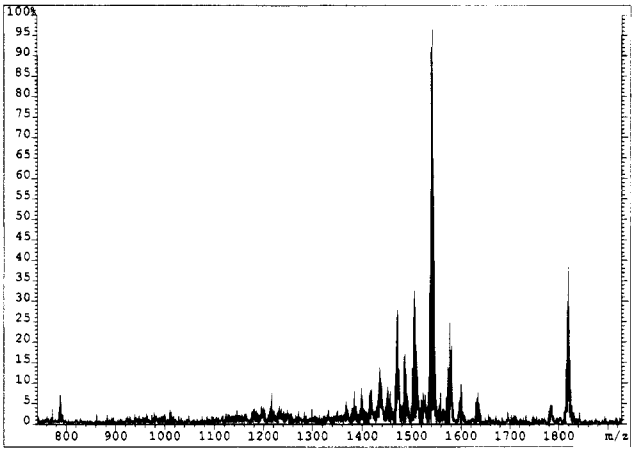


**Figure 1.** Negative LSIMS for $(n\text{-}Bu_4N)_2Re_6S_5OCl_8$. Peak assignment is given in Table 1.

peaks of the spectrum[7] correspond to the disubstituted cluster $(n\text{-}Bu_4N)_3[Re_6S_5Te_2Cl_7]$. This is taken as an indication that the latter is present in larger amounts when the reaction is carried out at higher temperatures. As of yet, this is the only indication in the series that double substitution may be achieved on the cluster core. All attempts to grow single crystals of either cluster salt from the product mixture failed which precluded any further characterization of these compounds.

**$(n\text{-}Bu_4N)Re_6Q_5Cl_9$ vs $[(CH_3)_3Si]_2O$ or $H_2O$.** The synthesis of **1** by reaction of $[(CH_3)_3Si]_2O$ with $(n\text{-}Bu_4N)Re_6S_5Cl_9$ and the subsequent determination of its crystal structure led us to realize that we had serendipitously obtained small amounts of this compound in earlier studies, albeit without identifying the presence of the oxygen atom on the cluster core, by refluxing the cluster monoanion in water.[8] It should be emphasized, however, that only the former reaction provides the oxo sulfido rhenium cluster as a *single product* in *high yields*.

It is of interest to note that $(n\text{-}Bu_4N)Re_6Se_5Cl_9$ does not react, either at room temperature with $[(CH_3)_3Si]_2O$ or refluxing conditions in water, to give an oxo seleno rhenium cluster. This finding is in contrast with the double substitution reaction in $DMF/H_2O$ solutions of the neutral cluster core $Re_6Se^i_4Cl^i_4(Cl^a_6)$ reported by Holm and co-workers.

**Liquid Secondary Ion Mass Spectrometry.** LSIMS, successfully used recently to characterize molybdenum halide cluster anions[9] and the rhenium chalcohalide cluster anions $(n\text{-}Bu_4N)_2Re_6Q_6Cl_8$,[3] proved to be an easy, efficent method for identifying these heterosubstituted all-inorganic cluster molecules. The results of these studies provide further support for the specificity of the one-inner chloride ligand substitution reaction since, with the exception of the telluride adducts of $Re_6S_5Cl_9^-$, only one singly substituted cluster form is present in the LSIMS in each case, in agreement with the elemental analyses results of single-crystals of **1**–**6**. A typical negative LSI mass spectrum is given for $(n\text{-}Bu_4N)_2[Re_6S_5OCl_8]$ in Figure 1. As exemplified in Figure 2 for the peak $[(Bu_4N)Re_6S_5OCl_8]^-$, there is a full agreement between the observed and calculated isotopic ion distributions. Similar spectra and agreements were consistently obtained throughout the series, hence, the formulations of the fragments and characteristic data for all compounds

(4) Fenske, D. in *Clusters and Colloids*, Schmid, G., Ed.; VCH: Weinheim, Germany **1994**; pp 212–298.

(5) (a) Gibson, V. C.; Kee, T. P.; Shaw, A. *Polyhedron* **1988**, *7*, 579–580. (b) Gibson, V. C.; Kee, T. P. *J. Chem. Soc., Chem. Commun.* **1989**, 656–657. (c) Hidalgo, G.; Pellinghelli, M. A.; Royo, P.; Serrano, R.; Tiripicchio, A. *J. Chem. Soc., Chem. Commun.* **1990**, 1118–119. (d) Herrmann, W. A.; Thiel, W. R.; Herdtweeck, E. *Chem. Ber.* **1990**, *123*, 271–276.

(6) *m/z*, assignment: 1931, $[(Bu_4N)Re_6S_5TeCl_8]$; 1747, $[Re_6S_5Te_2Cl_6]^-$; 1712, $[Re_6S_5Te_2Cl_5]^-$; 1689, $[Re_6S_5TeCl_8]^-$; 1654, $[Re_6S_5TeCl_7]^-$; 1619, $[Re_6S_5TeCl_6]^-$ and 845, $[Re_6S_5TeCl_8]^{2-}$.

(7) *m/z*, assignment: 2024, $[(Bu_4N)Re_6S_5Te_2Cl_7]^-$; 1989, $[(Bu4N)Re_6S_5Te_2Cl_6]^-$; 1782, $[Re_6S_5Te_2Cl_7]^-$; 1747, $[Re_6S_5Te_2Cl_6]^-$ and 1712, $[Re_6S_5Te_2Cl_5]^-$.

(8) Boubekeur, K. Thesis, Université de Rennes I, 1989.

(9) (a) Johnston, D. H.; Gaswick, D. C.; Lonergan, M. C.; Stern, C. L.; Shriver, D. F. *Inorg. Chem.* **1992**, *31*, 1869–1873. (b) Hodali, H. A.; Hung, H.; Shriver, D. F. *Inorg. Chim. Acta* **1992**, *198*–200, 245–248.

**Table 1.** Negative Ion LSIMS of $(n\text{-Bu}_4\text{N})_2\text{Re}_6\text{S}_5\text{OCl}_8$ (**1**), $(n\text{-Bu}_4\text{N})_2\text{Re}_6\text{S}_6\text{Cl}_8$ (**2**), $(n\text{-Bu}_4\text{N})_2\text{Re}_6\text{S}_5\text{SeCl}_8$ (**3**), $(n\text{-Bu}_4\text{N})_2\text{Re}_6\text{Se}_5\text{SCl}_8$ (**4**), $(n\text{-Bu}_4\text{N})_2\text{Re}_6\text{Se}_6\text{Cl}_8$ (**5**), and $(n\text{-Bu}_4\text{N})_2\text{Re}_6\text{Se}_5\text{TeCl}_8$ (**6**), $m/z$[a] (Relative Abundance, %)

| assignment | 1 | 2 | 3 | 4 | 5 | 6 |
|---|---|---|---|---|---|---|
| $[(\text{Bu}_4\text{N})\text{Re}_6\text{Q}_5\text{ECl}_8]^-$ | 1819.6 (68) | 1835.6 (28) | 1883.6 (43) | 2071.3 (12) | 2117.3 (25) | 2167.2 (36) |
| $[(\text{Bu}_4\text{N})\text{Re}_6\text{Q}_5\text{ECl}_7]^-$ | 1784.6 (12) | 1800.6 (3) | 1846.6 (4) | 2036.3 (2) | 2082.3 (2) | 2130.3 (6) |
| $[\text{Re}_6\text{Q}_5\text{ECl}_8]^-$ | 1577.3 (53) | 1593.3 (55) | 1641.3 (48) | 1829.0 (36) | 1875.0 (62) | 1925.0 (70) |
| $[\text{Re}_6\text{Q}_5\text{ECl}_7]^-$ | 1542.4 (100) | 1158.3 (100) | 1604.3 (100) | 1794.1 (100) | 1840.0 (100) | 1888.0 (100) |
| $[\text{Re}_6\text{Q}_5\text{ECl}_6]^-$ | 1505.4 (34) | 1521.4 (23) | 1569.3 (22) | 1757.1 (29) | 1805.0 (32) | 1853.0 (32) |
| $[\text{Re}_6\text{Q}_5\text{ECl}_5]^-$ | 1470.4 (25) | 1486.4 (15) | 1534.3 (11) | 1722.1 (26) | 1770.1 (19) | 1818.1 (19) |
| $[\text{Re}_6\text{Q}_5\text{ECl}_8]^{2-}$ | 788.7 (5) | 796.7 (7) | 820.6 (8) | 914.5 (2) | 937.5 (2) | 962.5 (15) |

[a] $m/z$ value of the most abundant ion in the isotopic distribution. Peaks above $m/z$ = 300 and greater than 2% are included.

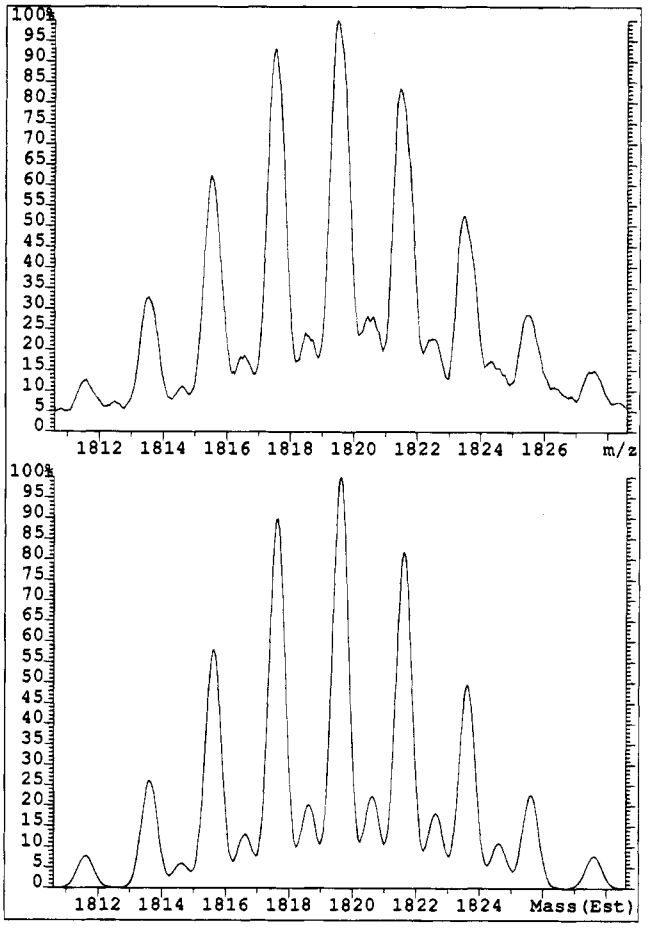


**Figure 2.** Observed (top) and calculated (bottom) isotopic ion distribution for the parent ion, $[(\text{Bu4N})\text{Re}_6\text{S}_5\text{OCl}_8]^-$, at $m/z$ = 1819.6.

**Table 2.** Negative Ion LSIMS of $(n\text{-Bu}_4\text{N})\text{Re}_6\text{Q}_5\text{Cl}_9$, $m/z$[a] (Relative Abundance, %)

| assignment | $(n\text{-Bu}_4\text{N})\text{Re}_6\text{S}_5\text{Cl}_9$ | $(n\text{-Bu}_4\text{N})\text{Re}_6\text{Se}_5\text{Cl}_9$ |
|---|---|---|
| $[\text{Re}_6\text{S}_5\text{Cl}_9]^-$ | 1596.3 (100) | 1832.0 (100) |
| $[\text{Re}_6\text{S}_5\text{Cl}_8]^-$ | 1561.3 (33) | 1797.1 (37) |
| $[\text{Re}_6\text{S}_5\text{Cl}_7]^-$ | 1526.4 (19) | 1762.1 (19) |
| $[\text{Re}_6\text{S}_5\text{Cl}_6]^-$ | 1489.4 (8) | 1725.1 (8) |

[a] $m/z$ value of the most abundant ion in the isotopic distribution. Peaks above $m/z$ = 300 and greater than 2% are included.

reported in Table 1. Also included in Table 2 are the data for the cluster monoanions, $(n\text{-Bu}_4\text{N})\text{Re}_6\text{Q}_5\text{Cl}_9$, which had not yet been reported.

The LSIM spectra of the series of cluster dianions in **1**–**6** exhibit the same characteristics with the highest mass peak corresponding to $[(\text{Bu}_4\text{N})\text{Re}_6\text{Q}_5\text{ECl}_8]^-$. All other peaks of the spectra are attributed to molecular cluster ions. In this second set of peaks, those with the highest $m/z$ proved to correspond to $[\text{Re}_6\text{Q}_5\text{ECl}_8]^-$ species formed by oxidation of $[\text{Re}_6\text{Q}_5\text{ECl}_8]^{2-}$ ions within the *m*-nitrobenzyl alcohol matrix under the LSIMS conditions.[10] $[\text{Re}_6\text{Q}_5\text{ECl}_8]^{2-}$ ions, however, are also observed in all the compounds studied, although in low relative abundance. Elimination of a chlorine atom from the divalent molecular species leads to the $[\text{Re}_6\text{Q}_5\text{ECl}_7]^-$ ion which constitutes the base peak in all cases. Further losses of chlorine atoms give rise to characteristic peaks whose intensity decreases as the number of chlorine atoms lossed is increased.

For the cluster monoanions in $(n\text{-Bu}_4\text{N})\text{Re}_6\text{Q}_5\text{Cl}_9$ (Q= S, Se), the highest mass and base peaks of spectra have been assigned as $[\text{Re}_6\text{Q}_5\text{Cl}_9]^-$. Peaks of low intensity due to loss of chlorine atoms are also observed.

Finally, small peaks at 16 mass units above the major peaks collected in Table 1 are occasionally observed and attributed to the addition of one oxygen atom from the matrix to the former fragments, in agreement with similar observations reported for the FAB–MS spectra of gold clusters[11] and other organometallic compounds.[12]

**Structural Correlations.** The unit cell parameters for **1**–**6** are compared in Table 3. While the chalcogenide-substituted tetrabutylammonium salts **2**–**6** are all isostructural, the oxo sulfido rhenium cluster salt $(n\text{-Bu}_4\text{N})_2[\text{Re}_6\text{S}_5\text{OCl}_8]$ has a different structure. Therefore, a full structure determination was achieved for **1** and **6** only, whose crystallographic data are given in Table 4. The salient structural features of the cluster motifs in **1** and **6** are compared in Table 5, which also include those for $(n\text{-Bu}_4\text{N})[\text{Re}_6\text{S}_5\text{Cl}_9]$,[1] $(n\text{-Bu}_4\text{N})[\text{Re}_6\text{Se}_5\text{Cl}_9]$,[8,14] $(n\text{-Bu}_4\text{N})_2[\text{Re}_6\text{Se}_6\text{Cl}_8]$,[2,8,13] and $(n\text{-Bu}_4\text{N})_3[\text{Re}_6\text{S}_7\text{Cl}_7]$.[1]

The cluster dianion $[\text{ReS}_5\text{OCl}_8]^{2-}$, shown in Figure 3, presents two unique structural features unprecedented in these series of hexanuclear chalcohalide rhenium clusters, be they molecular forms or connected within extended solids. First, this is the only example where a single inner ligand, the oxygen atom for that matter, is localized in the solid state. That is, the cluster motif does not reside on a center of symmetry in the crystal and the remaining $S^i_5Cl^i_2$ ligands are found to be equally disordered on the remaining seven $L^i$ sites only. Second, there is a strong contraction of the hexanuclear cluster face capped

(10) Reynolds, J. D.; Cook, K. D.; Burn, J. L. E.; Woods, C. *J. Am. Soc. Mass Spectrom.* **1992**, *3*, 113.
(11) Boyle, P. D.; Johnson, B. J.; Alexander, B. D.; Casalnuovo, J. A.; Gannon, P. R.; Johnson, S. M.; Larka, E. A.; Mueting, A. M.; Pignolet, L. H. *Inorg. Chem.* **1987**, *26*, 1346.
(12) Sharp, T. R.; White, M. R.; Davies, J. F.; Stang, P. J. *Org. Mass Spectrom.* **1984**, *19*, 107.
(13) The structure of the tetrabutylammonium salt $(n\text{-Bu}_4\text{N})_2[\text{Re}_6\text{Se}_6\text{Cl}_8]$, reported by Holm et al. (tetragonal unit cell, space group *I4/mmm*, $V$ = 2849.2(8) Å$^3$),[2] differs from that of the crystals obtained at room temperature in the present work. The latter is in turn identical to the structure determined earlier on crystals of $(n\text{-Bu}_4\text{N})_2[\text{Re}_6\text{Se}_6\text{Cl}_8]$ obtained by thermal reaction in water and which crystallize in a monoclinic unit cell, space group $P2_1/n$, $a$ = 12.833(2) Å, $b$ = 11.588(2) Å, $c$ = 18.562(6) Å, $b$ = 90.04(1)°, $V$ = 2760 Å$^3$. See ref 8 and: Boubekeur, K.; Lenoir, C.; Perrin, A.; Batail, P. Unpublished material. Perhaps, on account of the larger volume observed, the crystal synthesized by Holm's group could contain additional solvent molecules.
(14) Pénicaud, A.; Boubekeur, K.; Batail, P.; Canadell, E.; Auban-Senzier, P.; Jérome, D. *J. Am. Chem. Soc.* **1993**, *115*, 4101–4112.

**Table 3.** Room Temperature Unit Cell Parameters for **1**–**6**

| compound | *a*, Å | *b*, Å | *c*, Å | *β*, deg | *V*, Å$^3$ |
|---|---|---|---|---|---|
| $(n\text{-Bu}_4\text{N})_2\text{Re}_6\text{S}_5\text{OCl}_8$ (**1**) | 18.476(2) | 16.224(4) | 18.419(9) | 92.33(2) | 5516(3) |
| $(n\text{-Bu}_4\text{N})_2\text{Re}_6\text{S}_6\text{Cl}_8$ (**2**) | 12.444(6) | 11.820(7) | 18.492(6) | 90.44(3) | 2719(2) |
| $(n\text{-Bu}_4\text{N})_2\text{Re}_6\text{S}_5\text{SeCl}_8$ (**3**) | 12.468(1) | 11.830(1) | 18.526(4) | 90.42(1) | 2732(1) |
| $(n\text{-Bu}_4\text{N})_2\text{Re}_6\text{Se}_5\text{SCl}_8$ (**4**) | 12.829(1) | 11.594(2) | 18.589(2) | 90.00(1) | 2765 (1) |
| $(n\text{-Bu}_4\text{N})_2\text{Re}_6\text{Se}_6\text{Cl}_8$ (**5**) | 12.852(1) | 11.615(2) | 18.622(6) | 90.10(2) | 2779(1) |
| $(n\text{-Bu}_4\text{N})_2\text{Re}_6\text{Se}_5\text{TeCl}_8$ (**6**) | 12.929(2) | 11.580(4) | 18.681(2) | 90.09(1) | 2796(1) |

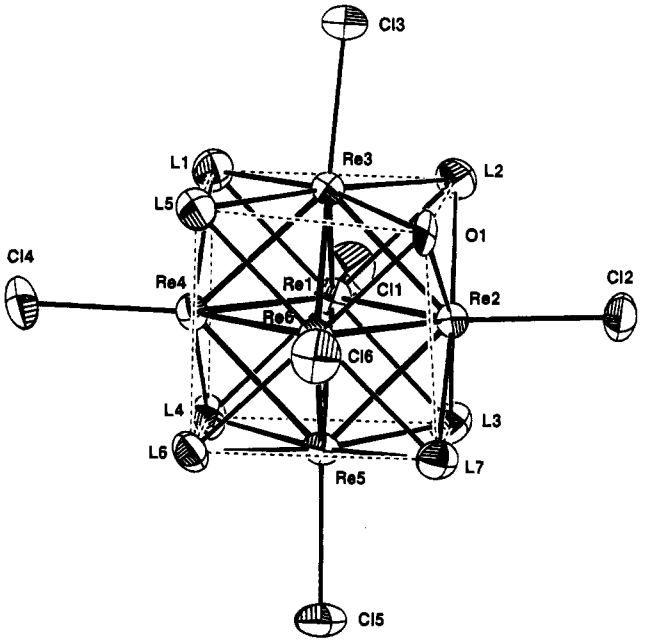


**Figure 3.** Structure of the $[Re_6S_5OCl_8]^{2-}$ anion, showing 50% probability ellipsoids and the atom labeling scheme. The dotted lines connecting the face-bridging ligand sites $L^i$ are meant to visualize better the distortion of the oxo sulfido cluster core.

**Table 4.** Crystallographic Data for $(n\text{-Bu}_4\text{N}_2\text{Re}_6\text{S}_5\text{OCl}_8$ (**1**) and $(n\text{-Bu}_4\text{N})_2\text{Re}_6\text{Se}_5\text{TeCl}_8$ (**6**)

| | **1** | **6** |
|---|---|---|
| formula | $C_{32}H_{72}Cl_8N_2ORe_6S_5$ | $C_{32}H_{72}Cl_8N_2Re_6Se_5Te$ |
| fw | 2062.1 | 2408.2 |
| *T*, K | 220 | 170 |
| cryst syst | monoclinic | monoclinic |
| space group | $P2_1/a$ | $P2_1/n$ |
| *a*, Å | 18.377(1) | 12.877(2) |
| b, Å | 16.138(6) | 11.312(8) |
| c, Å | 18.257(3) | 18.613(3) |
| *β*, deg | 92.16(1) | 90.11(1) |
| *V*, Å$^3$ | 5410(2) | 2711(2) |
| Z | 4 | 2 |
| *d*(calc), g·cm$^{-3}$ | 2.53 | 2.95 |
| *μ*, cm$^{-1}$ | 141.5 | 177.9 |
| R[a] | 0.044 | 0.045 |
| $R_w$[b] | 0.061 | 0.054 |
| goodness of fit, *S*[c] | 1.127 | 1.155 |

[a] $R = \Sigma||F_o| - |F_c||/\Sigma|F_o|$. [b] $Rw = [\Sigma w(|F_o| - |F_c|)^2/\Sigma w|F_o|^2]^{1/2}$; $w = [\sigma 2(I) + (pF_o^2)^2]^{-1}$. [c] $S = [\Sigma w(F_o^2 - F_c^2)^2/(n - \upsilon)]^{1/2}$.

with the single oxygen atom (Table 5), which gives rise to the distorted octahedral cluster core shown in Figure 3.

Within the crystals of $(n\text{-Bu}_4\text{N})_2\text{Re}_6\text{Se}_5\text{TeCl}_8$, the cluster motif is centrosymmetrical. Remarkably, in the solid state, two $L^i$ sites appear not to be occupied by a Te atom, all three Se, Te, and Cl atoms being disordered among the remaining six other $L^{i'}$ sites.

Finally, the present structure determinations indicate that the Re–Cl$^a$ distances are identical throughout the series of rhenium cluster dianions for a given core chalcogen (Table 5). This result adds substance to earlier correlations among the presently available structures of mono, di and trianions,[1] thereby clearly indicating that the Re–Cl$^a$ distance depends upon and is perhaps specific for the charge of the cluster motif.

**Molecular Orbital Considerations of the Cluster Charge-Dependent Re–Cl$^a$ Distances and the Oxo Cluster Core Distortion.** The chalcohalide rhenium cluster anions in this study can be incorporated into charge transfer salts with different organic donors.[14,15] The possibility now exists to manipulate this unique series of isosteric, isoelectronic, and isostructural anions with a range of different charges, all within a variety of isomers, which provides an exquisite opportunity for the construction of electroactive molecular solids. In order to understand the conducting or magnetic properties of these salts, it is essential to know the net negative charge of the cluster anions. Because of possible problems associated with the disorder on the face-capping sites (i.e. differently charged clusters could be found simultaneously in the same salt[16] ), it is very important to understand if there really is a correlation between the Re–Cl$^a$ distance and the charge of the cluster. If this is so, the occurrence of a Re–Cl$^a$ distance intermediate between those of Table 5 would be a serious warning about the possible existence of differently charged clusters occupying the same site in a given crystal structure. At this point, it is important to state that the situation is much more simple when attempting to understand the charge of organic donors from their internal geometry. In this case, the number of electrons of the species changes with the charge. Thus, a simple inspection of the nature of the HOMO (highest occupied molecular orbital) leads to an understanding of the correlation between the geometry and charge of the molecule. For the present clusters, the number of electrons is the same regardless of their charge. Therefore, if there is some electronic reason for the dependence of the Re–Cl$^a$ distance with the charge of the cluster, it is likely that it will not be concentrated on a single orbital but spread out among many of the occupied cluster orbitals. Because of the large number of isomers to be considered, a complete theoretical study with geometrical optimization of all the structures is not possible. A more simple way to tackle this problem is to perform calculations on model clusters built using a common geometry for the $Re_6L^i_8$ octahedral core and to study how the Re–Cl$^a$ overlap population changes with the ratio of the S and Cl atoms on the inner face-capping $L^i$ sites. Thus, we decided to carry out extended Hückel molecular orbital calculations for $Re_6S^i_4Cl^i_4(Cl^a_6)$, $[Re_6S^i_5Cl^i_3(Cl^a_6)]^-$, $[Re_6S^i_6Cl^i_2(Cl^a_6)]^{2-}$, $[Re_6S^i_7Cl^i(Cl^a_6)]^{3-}$, and $[Re_6S^i_8(Cl^a_6)]^{4-}$, as well as $[Re_6S^i_5O^iCl^i_2(Cl^a_6)]^{2-}$.

Because of the disorder on the inner ligand sites it is not easy to define a suitable geometrical model in order to perform

(15) (a) Batail, P.; Boubekeur, K.; Fourmigué, M.; Dolbecq, A.; Gabriel, J.-C.; Guirauden, A.; Livage, C.; Uriel, S. *New J. Chem.* **1994**, *18*, 999–1006 and references therein. (b) Boubekeur, K.; Lenoir, C.; Batail, P.; Carlier, R.; Tallec, A.; Le Paillard, M.-P.; Lorcy, D.; Robert, A. *Angew. Chem., Int. Ed. Engl.* **1994**, *33*, 1379–1381.

(16) (a) Batail, P.; Livage, C.; Parkin, S. S. P.; Coulon, C.; Martin, J. D.; Canadell, E. *Angew. Chem., Int. Ed. Engl.* **1991**, *30*, 1498. (b) Dolbecq, A. Thesis, Université de Paris-Sud, Orsay, 1995. Dolbecq, A.; Boubekeur, K.; Batail, P.; Canadell, E.; Auban-Senzier, P.; Coulon, C.; Lerstrup, K.; Bechgaard, K. *J. Mater. Chem.*, in press.

**Table 5.** Ranges and Mean Values of Interatomic Distances (Å) for the Cluster Motifs in $(n\text{-}Bu_4N)_2Re_6S_5OCl_8$, **1**, and $(n\text{-}Bu_4N)_2Re_6Se_5TeCl_8$, **6**, and Their Comparison to the Corresponding Data for $Re_6S_4Cl_{10}$,[1] $(n\text{-}Bu_4N)_2[Re_6S_5Cl_9]$,[1] $(n\text{-}Bu_4N)[Re_6Se_5Cl_9]$,[8] $(n\text{-}Bu_4N)_2[Re_6Se_6Cl_8]$,[8] and $(n\text{-}Bu_4N)_3[Re_6S_7Cl_7]$[1]

| compound | Re−Re | | Re−Cl$^a$ | | Re−L$^i$ | |
|---|---|---|---|---|---|---|
| | mean | range | mean | range | mean | range |
| $Re_6S_4Cl_{10}$ | 2.595(2) | 2.592(1)−2.599(1) | 2.319(11) | 2.301(6)−2.330(4) | 2.422(12) | 2.401(3)−2.447(3) |
| $(n\text{-}Bu_4N)Re_6S_5Cl_9]$ | 2.589(7) | 2.576(2)−2.607(2) | 2.344(45) | 2.288(12)−2.396(12) | 2.411(4) | 2.315(12)−2.513(13) |
| $(n\text{-}Bu_4N)_2[Re_6S_6Cl_8]$ | 2.573(8) | 2.562(1)−2.583(1) | 2.362(12) | 2.353(7)−2.375(4) | 2.401(9) | 2.384(5)−2.413(7) |
| $(n\text{-}Bu_4N)_3[Re_6S_7Cl_7]$ | 2.570(10) | 2.560(1)−2.581(1) | 2.397(3) | 2.396(10)−2.401(5) | 2.395(19) | 2.359(12)−2.422(7) |
| $(n\text{-}Bu_4N)_2[Re_6S_5OCl_8]$ | 2.587(9) | 2.573(1)−2.601(1) | 2.368(11) | 2.351(3)−2.377(5) | 2.415(11) | 2.435(5)−2.438(5) |
| for the oxygen-capped face | 2.523(8) | 2.516(1)−2.531(1) | | | 2.087(6)$^a$ | 2.08(1)−2.09(1)$^a$ |
| $(n\text{-}Bu_4N)_2[Re_6Se_6Cl_8]$ | 2.608(1) | 2.606(1)−2.612(1) | 2.378(1) | 2.372(4)−2.382(3) | 2.496(2) | 2.486(2)−2.507(2) |
| $(n\text{-}Bu_4N)_2[Re_6Se_5TeCl_8]$ | 2.618(4) | 2.6108(9)−2.6226(8) | 2.392(3) | 2.388(5)−2.394(3) | 2.536(28) | 2.490(2)−2.586(2) |

$^a$L = O.

the theoretical study. In fact, we carried out three types of calculations. In all of them we used a model cluster based on an ideal rhenium octahedron with identical Re−Re and Re−Cl$^a$ distances (2.595 Å and 2.319 Å, respectively, which are the average Re−Re and Re−Cl$^a$ distances in the neutral cluster, Table 5). The difference between the three series of calculations concerns the L$^i$ sites. In the first one, I, we used an ideal configuration with geometrically equivalent positions and two model ligands L and L′, whose 3s and 3p orbital exponents are identical and intermediate between those of Cl and S. The ionization potentials of the L$^i$ sites were those of the real atoms (see Experimental Section). In the second one (II), we used the same geometrical model but both the ionization potentials and the orbital exponents are those of the real S and Cl atoms. Finally, in the third one (III), the ionization potentials and the exponents are those of the real atoms and the geometric positions of the S and Cl atoms are different. These positions have been defined by taking the average of the distance of S and Cl to the center of the nearest triangular face in the neutral cluster. In every set of calculations, each of the isomers, that is with all different arrangements of the S and Cl atoms among the eigth available L$^i$ sites, were considered. Calculations in III are without any doubt closer to the real situation, but consideration of the II and I calculations is very important. They allow us to see if the calculated results can be structure dependent (through the actual positions of the S and Cl atoms or through their orbital extension given by the orbital exponents) or if they are intrinsic to the nature of the clusters. For instance, in I all the distances of a given type are identical as well as the orbital extension of the atoms on a given site, so that the only difference introduced in the calculation for the various clusters is the electronegativity of the different L$^i$ sites. Thus, if there is some trend in the overlap populations of the average Re−Cl$^a$ bonds, it has to be an intrinsic property of the ratio between the number of S and Cl atoms sharing the L$^i$ sites.

Our study for each cluster type involved the following steps. First, we enumerated the different possible isomers. Second, we calculated the energy and the average Re−Cl$^a$ overlap population for every isomer. Third, we calculated a thermalized average overlap population assuming that a Boltzmann distribution applies for the different isomers of a given cluster. Such a study was carried out following approaches I, II and III specified above. The main result of this study is that the thermalized average Re−Cl$^a$ overlap population clearly decreases with the increase of the cluster charge. This result is independent of the approach used in the calculations. For instance, the thermalized average Re−Cl$^a$ overlap populations were found to be 0.4576, 0.4507, 0.4450, 0.4405, and 0.4358 for the neutral, monovalent, divalent, trivalent and tetravalent clusters, respectively, within approach I, 0.4555, 0.4492, 0.4439, 0.4400 and 0.4358 within approach II, and 0.4588, 0.4514, 0.4445, 0.4390 and 0.4337 within approach III. These variations in overlap population are of the correct order of magnitude when compared with the variations in the Re−Cl$^a$ distances of Table 5. For instance, according to approach I, the average Re−Cl$^a$ overlap population decreases by 3.7% when going from the neutral to the trivalent cluster and the Re−Cl$^a$ average distance increases by 3.4%. The results are equally good for other approaches. This good agreement should not be overemphasized but it definitely suggests that our calculations are meaningful. In addition, the clear ordering of the Re−Cl$^a$ average overlap populations according to the charge of the cluster is not only found when the thermalized average overlap populations are considered, but also when looking at the average overlap populations of every isomer of all clusters. In view of all these results, we conclude that the lengthening of the Re−Cl$^a$ average distance with the charge is an intrinsic property of these clusters which only depends on the ratio of the S and Cl ligands on the inner (L$^i$) cluster sites. A likely reason for this correlation relies on the fact that there is more covalent mixing for the Re−S than for the Re−Cl bonds. Thus, when the number of sulfur ligands increases, the chlorine axial atoms can not as effectively compete for the Re valence orbitals so that the Re−Cl$^a$ overlap population decreases and the bond length increases.[17]

In order to further probe if the observed contraction of the Re−Re distances of the cluster face capped by the oxygen atom is electronic in origin, we carried out similar extended Hückel calculations for $[Re_6S^i_5O^iCl^i_2(Cl^a_6)]^{2-}$. It follows that the relative magnitude of the calculated Re−Re overlap populations of the two faces depends on the way the oxygen position is defined and in some instances is opposite to the observed trend in the experimental distances. This suggests that, at variance with the previous results, the deformation of the octahedra is not an intrinsic electronic property of the cluster and is essentially a size effect; i.e., the triangle of Re atoms near the oxygen compresses to interact better with the smaller O ligand. This is confirmed by analysis of the results for $[Re_6S_8Cl_6]^{4-}$ and $[Re_6S_7ClCl_6]^{3-}$ according to model I. In that case we simply increase the electronegativity of a L$^i$ site and, again, the change of the Re−Re overlap populations in the two faces is the opposite to that expected on the basis of the structure of $[Re_6S^i_5O^iCl^i_2(Cl^a_6)]^{2-}$. Thus, we conclude that the cluster core deformation in $[Re_6S^i_5O^iCl^i_2(Cl^a_6)]^{2-}$ is essentially governed by the smaller size of the O ligand.

## Conclusion

The reaction of $[(CH_3)_3Si]_2E$, E = O, S, Se, and Te, with $(n\text{-}Bu_4N)Re_6Q_5Cl_9$, Q = S and Se, proved to be an efficient cluster core ligand (L$^i$) substitution reaction which provides at

(17) We thank one reviewer for insightful comments on this point.

room temperature and high yields the tetrabutylammonium salts of the oxygen- or chalcogen-enriched, eventually heterosubstituted, hexanuclear molecular cluster dianions, $(n\text{-}Bu_4N)_2[Re_6S^i_5E^i\text{-}Cl^i_2(Cl^a_6)]$ (E = O, S, Se) and $(n\text{-}Bu_4N)_2[Re_6Se^i_5E^iCl^i_2(Cl^a_6)]$ (E = S, Se, Te). The latter have been fully characterized by liquid secondary negative ion mass spectrometry. While substitution of one inner chloride ligand of the cluster monoanions, $[Re_6Q^i_5Cl^i_3(Cl^a_6)]^-$, by either S, Se, or Te, leaves the octahedral $Re_6$ core undisturbed, there is a strong shrinking of the single octahedron face capped by the oxygen atom in the oxo sulfido rhenium cluster $[Re_6S_5OCl_8]^{2-}$. Furthermore, the determination of the $Re-Cl^a$ distances in the structure of $(n\text{-}Bu_4N)_2Re_6S_5OCl_8$ and $(n\text{-}Bu_4N)_2Re_6Se_5TeCl_8$ adds important data to earlier structural studies and confirms that this distance increases with the molecular cluster charge, as demonstrated by extensive structural correlation in the series of neutral and mono-, di-, and trianions of such molecular cluster forms. Molecular orbital calculations of the extended Hückel type conducted in a series of model cluster forms with a variety of different chalcogen/halogen proportion and net cluster charges, $Re_6S^i_4Cl^i_4(Cl_6)$, $[Re_6S^i_5Cl^i_3(Cl^a_6)]^-$, $[Re_6S^i_6Cl^i_2(Cl^a_6)]^{2-}$, $[Re_6S^i_7\text{-}Cl^i(Cl^a_6)]^{3-}$, and $[Re_6S^i_8(Cl^a_6)]^{4-}$, as well as $[Re_6S^i_5O^iCl^i_2(Cl^a_6)]^{2-}$, demonstrate that the thermalized average $Re-Cl^a$ overlap population decreases with the increase in cluster charge, a genuine electronic effect which qualifies the actual $Re-Cl^a$ distance in a given structure as specific to the cluster anion charge. On the contrary, the shrinking of the oxo-capped $Re_3$ face is not an electronic effect but more the result of a steric adjustment.

The construction of cation radical salts based on these heterosubstituted cluster anions is being pursued in order to create situations where small but significant modifications of the chalcogen nature and proportions on the cluster site, as well as the presence of a single oxygen atom, may affect the intermolecular interactions and cooperative electronic response within highly ordered networks in the solid state.

## Experimental Section

$(n\text{-}Bu_4N)Re_6Q_5Cl_9$ (Q = S, Se) were prepared as described previously.[1,14] $[(CH_3)_3Si]_2O$ and $[(CH_3)_3Si]_2S$ were purchased from commercial sources. $[(CH_3)_3Si]_2Se$ and $[(CH_3)_3Si]_2Te$ were synthesized as described by Detty and Seidler.[18]

**General Procedure.** A suspension of $(n\text{-}Bu_4N)Re_6Q_5Cl_9$ (Q = S, Se) (30 mg, ca. 15 $\mu$mol) in neat acetonitrile (20 mL) was treated with freshly distilled $[(CH_3)_3Si]_2E$, (E = O, S, Se, Te) (ca. 150 $\mu$mol), under an argon atmosphere at room temperature. Note that since $[(CH_3)_3Si]_2Te$ is light sensitive, the vessel should be wrapped in foil. The reactions were stirred for 4 h at room temperature to give clear orange solutions as well as a grey precipitate of Se or Te. An excess of solid tetrabutylammonium chloride was then added and the solutions were stirred for 1 h. The solutions were filtered off to eliminate Se or Te and evaporated in vacuo to dryness. Orange residues were washed with ethanol to eliminated the excess of tetrabutylammonium chloride and recrystallized from acetonitrile (ca. 5 mL) to yield beautiful ruby red octahedral crystals of excellent X-ray quality.

**$(n\text{-}Bu_4N)_2[Re_6S_5OCl_8]$ (1).** A 30 mg yield of **1** was obtained out of 30 mg of $(n\text{-}Bu_4N)Re_6S_5Cl_9$ (yield 89%). Anal. Calcd for $C_{32}H_{72}N_2Re_6S_5OCl_8$ (2062.1): C, 18.64; H, 3.52; N, 1.36; S, 7.70; Cl, 13.75. Found: C, 18.49; H, 3.26; N, 1.3; S, 7.66; Cl, 13.87.

**$(n\text{-}Bu_4N)_2[Re_6S_6Cl_8]$ (2).** A 26 mg yield of **2** was obtained out of 30 mg of $(n\text{-}Bu_4N)Re_6S_5Cl_9$ (yield 77%). Anal. Calcd for $C_{32}H_{72}N_2Re_6S_6Cl_8$ (2078.1): C, 18.49; H, 3.49; N, 1.35; S, 9.26; Cl, 13.65. Found: C, 18.21; H, 3.21; N, 1.57; S, 9.24; Cl, 13.49.

**$(n\text{-}Bu_4N)_2[Re_6S_5SeCl_8]$ (3).** A 22 mg yield of **3** was obtained out of 30 mg of $(n\text{-}Bu_4N)Re_6S_5Cl_9$ (yield 63%). Anal. Calcd for $C_{32}H_{72}N_2Re_6S_5SeCl_8$ (2125.1): C, 18.09; H, 3.42; N, 1.32; S, 7.54; Cl, 13.35. Found: C, 18.23; H, 3.12; N, 1.62; S, 7.52; Cl, 13.22.

**$(n\text{-}Bu_4N)_2[Re_6Se_5SCl_8]$ (4).** A 27 mg sample of **4** was obtained out of 30 mg of $(n\text{-}Bu_4N)Re_6Se_5Cl_9]$ (yield 81%). Anal. Calcd for $C_{32}H_{72}N_2Re_6Se_5SCl_8$ (2312.6): C, 16.62; H, 3.14; N, 1.21; Cl, 12.26. Found: C, 16.47; H, 2.99; N, 1.51; Cl, 12.11.

**$(n\text{-}Bu_4N)_2[Re_6Se_6Cl_8]$ (5).** A 25 mg sample of **5** was obtained out of 30 mg of $(n\text{-}Bu_4N)Re_6Se_5Cl_9$ (yield 73%). Anal. Calcd for $C_{32}H_{72}N_2Re_6Se_6Cl_8$ (2359.5): C, 16.29; H, 3.08; N, 1.19; Cl, 12.02. Found: C, 16.36; H, 2.99; N, 1.45; Cl, 12.02.

**$(n\text{-}Bu_4N)_2[Re_6Se_5TeCl_8]$ (6).** A 22 mg sample of **6** was obtained out of 30 mg of $(n\text{-}Bu_4N)Re_6Se_5Cl_9$ (yield 63%). Anal. Calcd for $C_{32}H_{72}N_2Re_6Se_5TeCl_8$ (2408.2): C, 15.96; H, 3.01; N, 1.16; Cl, 11.78. Found: C, 16.14; H, 2.81; N, 1.31; Cl, 11.56.

**Liquid Secondary Ion Mass Spectrometry.** The compounds were analyzed at the University of Zaragoza by using liquid secondary ion mass spectrometry (LSIMS). Negative LSIM spectra were recorded on a VG-Autospec (VG Analytical Manchester, UK) high resolution trisector EBE mass spectrometer. Ions were produced by a 30 keV primary beam of cesium ions, extracted and accelerated by a 8 kV potential. Samples were dissolved in acetonitrile and mixed with the *m*-nitrobenzyl alcohol matrix on the target. Scans were obtained in the 3000–300 mass range at *ca.* 1500 resolving power (measured as peak width at 5% height) and at a scan rate of 10 s decade$^{-1}$. Mass calibration was achieved with the use of reference spectra of cesium iodide and a maximum error of 0.3 mass unit was obtained. Data procesing was achieved using the VG-OPUS v2.1 software running on a DEC VAX 3100 workstation. Spectra reported are the average of at least 10 scans. The calculated isotopic ion distributions are based on the following natural isotopic abundances: $^{185}$Re, 37.40%; $^{187}$Re, 62.60%; $^{35}$Cl, 75.77%; $^{37}$Cl, 24.23%; $^{32}$S, 95.02%; $^{33}$S, 0.75%; $^{34}$S, 4.21%; $^{36}$S, 0.02%; $^{74}$Se, 0.90%; $^{76}$Se, 9.00%; $^{77}$Se, 7.60%; $^{78}$Se, 23.50%; $^{80}$Se, 49.60%; $^{82}$Se, 9.40%; $^{120}$Te, 0.10%; $^{122}$Te, 2.60%; $^{123}$Te, 0.91%; $^{124}$Te, 4.82%; $^{125}$Te, 7.14%; $^{126}$Te, 18.95%; $^{128}$Te, 31.69%; $^{130}$Te, 33.80%; $^{16}$O, 99.76%; $^{17}$O, 0.04%; $^{18}$O, 0.20%.

**X-ray Crystallography.** Experimental details for compounds **1** and **6** are given in Table 4. In each case a suitable single crystal was mounted on a glass fiber in a random orientation. Preliminary examination and data collection were performed on a $\kappa$-axis Enraf-Nonius CAD4-F diffractometer using graphite monochromatized Mo K$\alpha$ radiation. Unit cell dimensions and crystal orientation matrix were derived from least-squares refinement of setting angles of 25 reflections. Intensity data were collected using $\omega-2\theta$ scan mode. Data were corrected for background, Lorentz, polarization, and absorption effects. The structures were solved by direct methods and refined (on *F*'s) by full-matrix least-squares calculations initially with isotropic and finally with anisotropic thermal parameters for non H-atoms. The atomic scattering factors and anomalous dispersion corrections were taken from ref 23. All calculations were performed on a DEC microVAXII and IBM RS/6000 computers by using the Enraf–Nonius SDP/PLUS[19] and XTAL3.2[20] systems of programs.

**Structure Solution.** (a) **$(n\text{-}Bu_4N)_2[Re_6S_5OCl_8]$ (1).** A tabular ruby red crystal with dimensions 0.16 × 0.16 × 0.15

(18) Detty, M. R.; Seidler, M. D. *J. Org. Chem.* **1982**, *47*, 1354–1356.

$mm^3$ was used. A total of 12 182 intensities were recorded ($\theta \leq 27°$) at 240 K in the quadrants $+h,+k,\pm l$. An absorption correction based on DIFABS procedure was applied (correction factors ranged from 0.863 to 1.136) to the reflection data. Data reduction and averaging yielded 11197 independent reflections ($R_{int}$=0.026) of which 5174, with $I \geq 3\sigma(I)$, were used for the calculations. Systematic extinctions were consistent with the unambiguous space group $P2_1/a$. The structure was solved by direct methods. All non-H atoms of the structure were refined anisotropically. The asymmetric unit consists of one cluster anion and two tetrabutylammonium cations, all these ions being located in general position. Except for the oxygen atom, which is perfectly ordered, the other cluster core face-capping atoms are disordered. It was thus assumed that these sites are shared by S and Cl atoms with a statistical occupancy of 5/7 and 2/7 respectively. In the last refinement cycles these positions were refined independently.

**(b) ($n$-$Bu_4N$)$_2$[$Re_6Se_5TeCl_8$] (6).** A tabular dark red crystal with dimensions 0.12 × 0.12 × 0.09 $mm^3$ was used. A total of 6182 intensities were recorded ($\theta \leq 27°$) at low temperature (170K) in the quadrants $+h,+k,\pm l$. An empirical absorption correction based on the DIFABS procedure was applied (correction coefficients ranged from 0.847 to 1.311) to the reflection data. Data reduction and averaging yielded 5918 independent reflections ($R_{int}$ = 0.044) of which 2797 had $I \geq 3\sigma(I)$ and were used for the calculations. Systematic extinctions were consistent with the unambiguous space group $P2_1/n$. The structure was solved by direct methods which revealed three independent rhenium atoms in general positions. The remaining atoms were found on successive difference Fourier maps. All atoms were refined anisotropically except hydrogen atoms which were introduced in structure factors calculations with a common overall isotropic temperature factor and not refined. The asymmetric unit consists of half of a cluster anion located on an inversion center and one tetrabutylammonium cation in a general position. The cluster core face-capping sites are shared by Se, Cl, and Te atoms with statistical occupancies of $^5/_8$, $^2/_8$ and $^1/_8$, respectively, if one assumes a fully disordered situation. With the sum of the populations of the three atom types constrained to be one on any position, the site occupation factor values are found to be identical to the theoretical ones for two out of the four independent sites. For the third position, the proportions of Cl and Te are respectively half and double the theoretical values. The fourth position is free of Te and occupied by approximately half of a Se and half of a Cl. Thus, the sum of the atom populations on the eight inner cluster sites corresponds to the formulation $Se_5TeCl_2$ in agreement with the elemental analysis and mass spectrometry results.

**Molecular Orbital Calculations.** The calculations were of the extended Hückel type[21] and the modified Wolfsberg–Helmholz formula[22] was used to calculate the non diagonal $H_{ij}$ matrix elements. The exponents and the diagonal $H_{ii}$ values (eV) used were 2.356 and −26.3 for Cl 3s, 1.733 and −14.0 for Cl 3p, 2.122 and −20.0 for S 3s, 1.827 and −11.0 for S 3p, 2.275 and −32.3 for O 2s, 2.275 and −14.8 for O 2p, and 2.398 and −9.36 for Re 6p. The 5d orbitals of Re were written as a linear combination of two Slater type orbitals. The $H_{ii}$ value, exponents ($\zeta_a$ and $\zeta_b$) and contraction coefficients ($c_a$ and $c_b$) used were −12.66, 5.343, 2.277, 0.6377, and 0.5657, respectively. In some of the calculations an average ligand L, with exponents and parameters as specified in the discussion, was used.

**Acknowledgment.** We thank the CNRS-PIRMAT for support and the European Union Human Capital and Mobility Program for a postdoctoral fellowship (S.U.).

**Supporting Information Available:** Tables of atomic coordinates, bond distances, bond angles, and thermal parameters, and drawing showing atom numbering schemes (31 pages). Ordering information is given on any current masthead page.

IC950041+

(19) *Structure Determination Package SDP/VAX V. 3.0 User's Guide*; Enraf-Nonius: Delft, The Netherlands, 1985.
(20) S. R. Hall, H. D. Flack, J. M. Stewart, *XTAL 3.2 Reference Manual*; Universities of Western Australia, Geneva and Maryland, 1992.
(21) Hoffmann, R. J. *J. Chem. Phys.* **1963**, *39*, 1397.
(22) Ammeter, J.; Bürgi, H.-B.; Thibeault, J.; Hoffmann, R. J. *J. Am. Chem. Soc.* **1978**, *100*, 3686.
(23) *International Tables for X-ray Crystallography*; The Kynoch Press: Birmingham, England, 1974.